Annexation of a High-Activity Enzyme in a Synthetic Three-Enzyme Complex Greatly Decreases the Degree of Substrate Channeling

ARTICLE *in* ACS SYNTHETIC BIOLOGY · NOVEMBER 2013

Impact Factor: 4.98 · DOI: 10.1021/sb4000993 · Source: PubMed

ACS SyntheticBiology

Research Article

pubs.acs.org/synthbio

Annexation of a High-Activity Enzyme in a Synthetic Three-Enzyme Complex Greatly Decreases the Degree of Substrate Channeling

Chun You[†] and Y.-H. Percival Zhang[†,‡,§,*]

[†]Biological Systems Engineering Department, Virginia Tech, 304-A Seitz Hall, Blacksburg, Virginia 24061, United States of America

[‡]Cell-Free Bioinnovations Inc., 2200 Kraft Drive, Suite 1200B, Blacksburg, Virginia 24060, United States of America

[§]Gate Fuels Inc., Blacksburg, Virginia 24060, United States of America

Supporting Information

ABSTRACT: The self-assembled three-enzyme complex containing triosephosphate isomerase (TIM), aldolase (ALD), and fructose 1,6-biphosphatase (FBP) was constructed via a mini-scaffoldin containing three different cohesins and the three dockerin-containing enzymes. This enzyme complex exhibited 1 order of magnitude higher initial reaction rates than the mixture of noncomplexed three enzymes. In this enzyme cascade reactions, the reaction mediated by ALD was the rate-limiting step. To understand the in-depth role of the rate-limiting enzyme ALD in influencing the substrate channeling effect of synthetic enzyme complexes, low-activity ALD from *Thermotoga maritima* was replaced with a similar-size ALD isolated from *Thermus thermophilus*, where the latter had more than 5 times specific activity of the former. The synthetic three-enzyme complexes annexed with either low-activity or high-activity ALDs exhibited higher initial reaction rates than the mixtures of the two-enzyme complex (TIM-FBP) and the nonbound low-activity or high activity ALD at the same enzyme concentration. It was also found that the annexation of more high-activity ALD in the synthetic enzyme complexes drastically decreased the degree of substrate channeling from 7.5 to 1.5. These results suggested that the degree of substrate channeling in synthetic enzyme complexes depended on the enzyme choice. This study implied that the construction of synthetic enzyme enzymes in synthetic cascade pathways could be a very important tool to accrelerate rate-limiting steps controlled by low-activity enzymes.

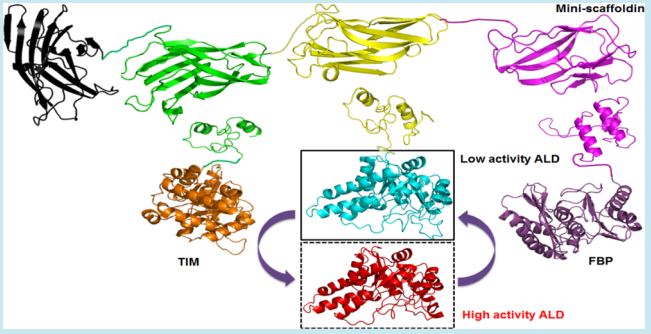

KEYWORDS: *enzyme cascade, rate-limiting step, cell-free synthetic biology, substrate channeling, metabolon, synthetic enzyme complex*

Synthetic biology is bringing engineering design principles to biological systems. The primary goal of synthetic biology is the design and construction of new biological functions and systems better than their natural counterparts or even non-natural ones, for example, enzymatic conversion of beta-1,4-glucosidic bond-linked cellulose to α-1,4-glucosidic bond-linked starch.[1] These biological systems are generally constructed from parts to modules to pathways to systems. The vision and outcomes of synthetic biology could influence many other scientific and engineering fields as well as various aspects of daily life and society.[2] Although it receives less attention compared to in vivo synthetic biology, cell-free synthetic biology is essentially vital to the synthesis of special proteins and polysaccharides, as well as the economical production of biofuels, biochemical, and potential food/feed from biomass sugars.[3−8]

Inspired by natural multienzyme complexes, building synthetic enzyme complexes containing multiple cascade enzymes as building modules is a powerful tool in synthetic biology regardless of them occurring *in vivo* or *in vitro*. Such synthetic enzyme complexes can be constructed by gene fusion, coimmobilization, coentrapment, and scaffold-mediated assembly.[9] Recently, scaffold-mediated assembly received more and more attentions due to their features: high-retaining enzyme activity, flexible engineering ability for multimeric proteins, and assembly *in vivo* or *in vitro*.[10] Scaffolding templates used for synthetic enzyme complexes include DNA,[11−15] RNA,[16] and proteins.[17−19] Protein-based scaffoldins may be more advantageous in cell-free biosystems for advanced biomanufacturing than DNA or RNA-based scaffolds because they are less costly and can be produced on large scales.[20]

Synthetic enzyme complexes mediated by scaffoldins could facilitate substrate channeling, which is a process of transferring the product of one enzyme to an adjacent cascade enzyme without full equilibration with the bulk phase.[10,21] The associated benefits of substrate channeling include the protection of unstable intermediates, the forestallment of substrate competition among different pathways, the mitigation of toxic metabolite inhibition, the conversation of energy stored

Special Issue: Cell-Free Synthetic Biology

Received: July 31, 2013

   dx.doi.org/10.1021/sb4000993 | *ACS Synth. Biol.* XXXX, XXX, XXX−XXX

in glycosidic bonds, etc.[10,18,22−26] For example, Keasling and his co-workers demonstrated to optimize the stoichiometry of the three-enzyme complex organized by scaffoldins to rapidly remove toxic metabolites in the in vivo synthetic pathway. As a result, the product titer was increased by 77 folds with low enzyme expression and reduced metabolic load.[18] In our previous study, an *in vitro* synthetic three-enzyme complex containing triosephosphate isomerase (TIM, EC 5.3.1.1), aldolase (ALD, EC 4.1.2.13), and fructose 1,6-bisphosphatase (FBP, EC3.1.3.11) was constructed by using cohesins and dockersin from cellulosomes, and this enzyme complex showed more than 1 order of magnitude higher initial reaction rates than that of the noncomplexed enzyme mixture.[25] In this enzyme complex, the reaction mediated by ALD from *Thermotoga maritima* (TmALD) was the rate-limiting step because its specific activity (i.e., 0.2 U/mg in the aldol condensation direction) was approximately two and four order magnitudes lower than those of FBP (i.e., 18.7 U/mg) and of TIM (i.e., > 3000 U/mg), respectively.[27] Although the degree of substrate channeling of the enzyme complex relative to the noncomplexed enzyme mixture was reported to be related to the linker length, enzyme orientation, and scaffold stoichiometry,[20,21] the choice of enzymes especially responsible for catalyzing the rate-limiting step in synthetic enzyme complexes, was not investigated in a single-factor experiment.

Not all of synthetic enzyme complexes exhibit enhanced reaction rates compared with their noncomplexed enzyme mixture counterparts. For example, a three-enzyme complex linked together by using non-natural amino acid incorporation, heterobifunctional linkers, and azide−alkyne cycloaddtion exhibited comparable kinetic behaviors with the uncoupled enzymes.[28] In the enzymatic conversion of cellulose to starch, the synthetic two-enzyme complex containing cellobiose phosphorylase and α-glucan phosphorylase had the same reaction rate as that of their simple enzyme mixture.[1] In this study, we discovered a new ALD whose activity in the aldol condensation direction is about 5 times higher than that of TmALD, and investigated the influence of the annexation of this enzyme into the TIM-ALD-FBP complex on the degree of substrate channeling in the single-factor experiment (Figure 1).

RESULTS AND DISCUSSION

Discovery of a Highly Active ALD. ALD, TIM, and FBP are cascade enzymes in the glycolysis and gluconeogenesis pathways. TIM catalyzes the reversible conversion of glyceraldehyde-3-phosphate (G3P) to dihydroxyacetone phosphate (DHAP). ALD catalyzes the reversible aldol condensation of G3P and DHAP to fructose 1,6-bisphosphate (F16P). FBP catalyzes the irreversible conversion of F16P to fructose 6-phosphate (F6P) (Scheme 1). These enzymes are also the key enzymes for cell-free production of high-yield hydrogen from a variety of sugars.[29−31] Because it had a specific activity of 0.22 U/mg in the aldol condensation direction at 60 °C, much lower than TIM from *Thermus thermophilus* (3500 U/mg) and FBP from *T. maritima* (18.7 U/mg) at 60 °C,[27] TmALD catalyzed the rate-limiting step when three enzymes had a molar ratio of 1:1:1. To increase overall reaction rates when using decreased protein loadings, it was vital to discover more active enzyme building blocks.

By searching enzyme database (BRENDA) for published enzyme characteristics, we found that ALD from *Thermus aquaticus* (TaALD) had a very high specific activity of 46 U/mg at 70 °C on the direction of F16P cleavage.[32] Unfortunately,

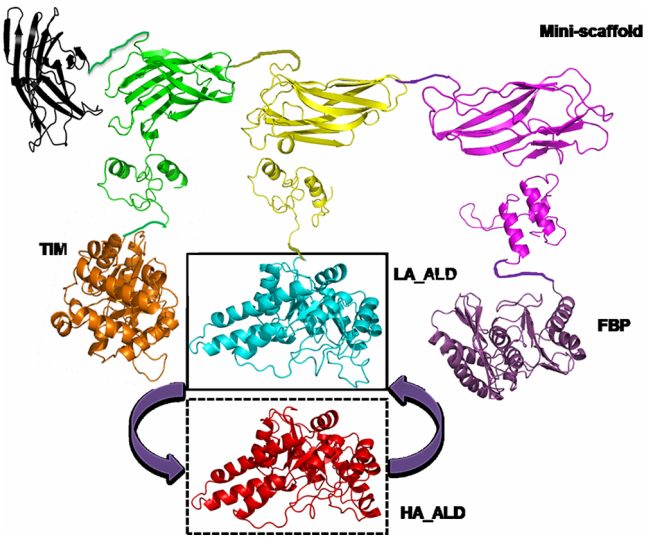

Figure 1. Schematic representation of the self-assembled three-enzyme complex containing TIM-CtDoc, LA_ALD-CcDoc, FBP-RfDoc, and a mini-scaffodlin containing three different types of cohesins and one family 3 carbohydrate-binding module. In it, LA_ALD could be replaced with another high-activity ALD (HA_ALD). Here, each pair of the matching cohesin and dockerin is presented in the same color.

Scheme 1. Cascade Reactions Catalyzed by the Enzymes TIM, ALD, and FBP, in Which the Reaction Mediated by ALD Was the Rate-Limiting Step

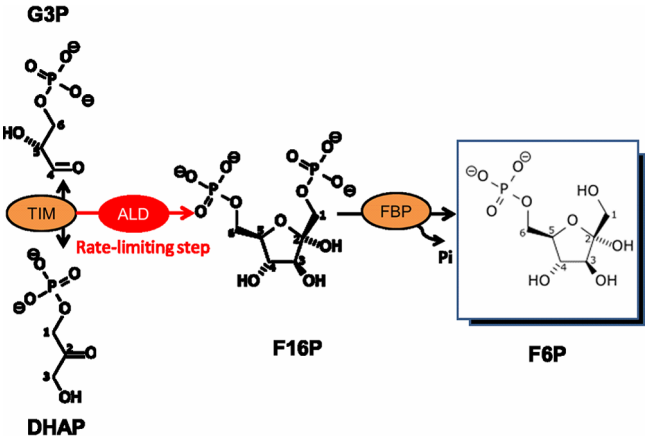

the genomic DNA of *T. aquaticus* is not available in our laboratory. Comparing the amino acid sequence of the open reading frame TTC1414, which was annotated to encode a putative ALD in *Thermus thermophilus*, with that of TaALD, we found that the sequence identity of TtcALD and TaALD was 92%, whereas the sequence identity of TmALD and TaALD was only 51% (Supporting Information Figure 1). Therefore, we hypothesized that TtcALD may be a high-activity ALD. After cloning, expression in *E. coli* and purification, the specific activity of the purified TtcALD was about 1.1 U/mg at 60 °C in the aldol condensation direction, approximately five times higher than that of TmALD.

Construction of Synthetic Enzyme Complex Containing High-Activity ALD. To understand the in-depth mechanism of the substrate channeling occurring in the TIM-ALD-FBP enzyme complex, we attempted to investigate the influence of the annexation of high-activity TtcALD (HA_ALD) into the TIM-ALD-FBP complex on the degree

dx.doi.org/10.1021/sb4000993 | ACS Synth. Biol. XXXX, XXX, XXX−XXX

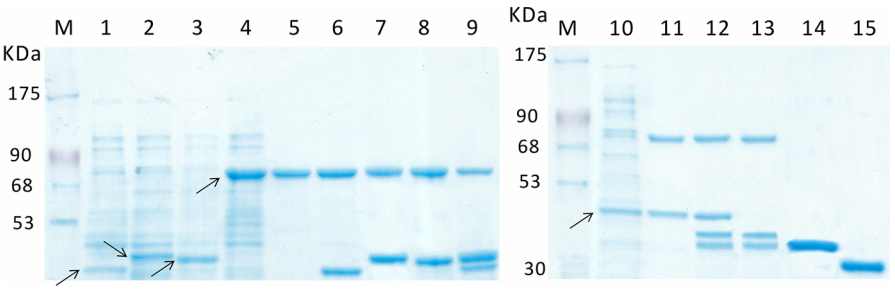

Figure 2. SDS-PAGE analysis of the enzyme complexes and purified LA_ALD and HA_ALD. Lane M, protein marker; Lanes 1−4, cell extract containing TIM-CtDoc, HA_ALD-CcDoc, FBP-RfDoc, and CBM-Scaf3 (i.e., CBM3-CtCoh-CcDoc-RfCoh), respectively; Lane 5, RAC adsorbed CBM-Scaf3; Lanes 6−8, RAC adsorbed CBM-Scaf3 and TIM-CtDoc, HA_ALD-CcDoc, and FBP-RfDoc, respectively; Lane 9, RAC adsorbed CBM-Scaf3, TIM-CtDoc, HA_ALD-CcDoC, and FBP-RfDoc; Lane 10, cell extract containing LA_ALD-CcDoc; Lane 11, RAC adsorbed CBM-Scaf3 and LA_ALD-CcDoc; Lane 12, RAC adsorbed CBM-Scaf3, TIM-CtDoc, LA_ALD-CcDoC, and FBP-RfDoc; Lane 13, RAC adsorbed CBM-Scaf3, TIM-CtDoc and FBP-RfDoc; Lane 14, purified dockerin-free LA_ALD; Lane 15, purified dockerin-free HA_ALD.

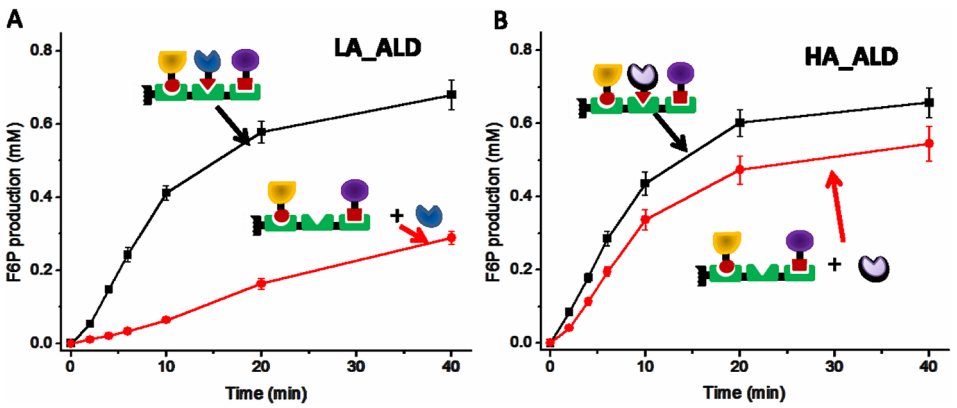

Figure 3. Profiles of F6P production catalyzed by 2 μM of the three-enzyme complexes and the mixture of the two-enzyme complex with the nonbound low activity ALD (A) and high activity ALD (B).

of substrate channeling. The synthetic mini-scaffoldin (CBM-Scaf3) was constructed to contain a family 3 cellulose-binding module (CBM3) at the N-terminus followed by three different type cohesins from the *Clostridium thermocellum* ATCC 27405 CipA, *Clostridium cellulovorans* ATCC 35296 CbpA, and *Ruminococcus flavefaciens* ScaB[25] (Figure 1). The dockerin-containing TIM, HA_ALD, and FBP were constructed by the addition of CtDoc from *C. thermocellum* CelS, CcDoc from *C. cellulovorans* EngE, and RfDoc from *R. flavefaciens* ScaA at their C-terminus, respectively (Figure 1). The addition of a dockerin to TIM, ALD, and FBP did not influence their activity (data not shown), as reported elsewhere.[17] The four *E. coli* BL21 strains harboring the expression plasmids expressed soluble recombinant proteins separately. When the four cell extracts were mixed together, the high-specificity interaction between cohesins and dockerins allowed each pair of cohesin and dockerin to bind tightly at the molar ratio of 1:1,[33] forming the synthetic three-enzyme complex (Figure 1). In the presence of solid regenerated amorphous cellulose (RAC), the synthetic three-enzyme complex was adsorbed on the surface of cellulosic material through a CBM3 in the mini-scaffoldin. After washing and centrifugation, the synthetic three enzyme complex was purified and immobilized on RAC, as described previously.[17] RAC, which was made through cellulose dissolution and regeneration in water, has a large-surface external area, different from other adsorbents whose surface areas are internal.[34,35]

SDS-PAGE analysis was conducted to check protein expression and purification (Figure 2). Four *E. coli* cell extracts containing TIM-CtDoc, HA_ALD-CcDoc, FBP-RfDoc, and CBM-Scaf3 were shown in Lanes 1−4 of Figure 3, respectively. The scaffoldin was purified by RAC pull-down experiment (Lane 5, Figure 2). When RAC was mixed with the cell extract containing the scaffoldin and another cell extract containing TIM-CtDoc, HA_ALD-CcDoc, or FBP-RfDoc, the high-affinity interaction between the cohesin and dockerin resulted in the formation of the unifunctional enzyme complex containing one scaffoldin and one dockerin-containing enzyme, exhibiting two bands in SDS-PAGE analysis (Lane 6−8, Figure 2). When RAC was mixed with the four cell extracts, the synthetic three-enzyme complex (i.e., TIM-HA_ALD-FBP) was formed and purified,[17] exhibiting three bands in SDS-PAGE (Lane 9, Figure 2) because the bands representing HA_ALD-CcDoc and FBP-RfDoc overlapped together due to their close molecular weights. The intensity of the overlaid band reflected by HA_ALD-CCDoc and FBP-RfDoc was about 2-fold of the band of TIM-CtDoc, suggesting that one scaffoldin can bind one TIM, one HA_ALD and one FBP, as reported previously.[25] Similarly, the three-enzyme complex containing low activity TmALD (LA_ALD) was self-assembled as described previously,[25] where one scaffoldin can bind one TIM, one LA_ALD and one FBP (Lane 12, Figure 2).

The enzyme activities of dockerin containing enzymes (TIM-CtDoc, HA_ALD-CcDoc, LA_ALD-CcDoc, FBP-RfDoc, Lane 6−8, Lane 11, Figure 2) that were attached to scaffoldin were the same with their dockerin-free counterparts. These results were consistent with those in a previous study.[36]

Substrate Channeling of Two Enzyme Complexes. To study the degree of substrate channelling of the three-enzyme

dx.doi.org/10.1021/sb4000993 | *ACS Synth. Biol.* XXXX, XXX, XXX−XXX

complexes relative to the two-enzyme complexes with dockerin-free ALD, the two-enzyme complex (TIM-FBP) was prepared by mixing the three cell extracts containing mini-scaffoldin, TIM-CtDoC, and FBP-RfDoc with the help of RAC. The TIM-FBP complex was purified to homogeneity (Lane 13, Figure 2). Two dockerin-free C-terminal His tagged ALDs were purified by Ni-NTA resins (Lane 14 and 15, Figure 2).

The F6P formation profiles were examined on 2.5 mM G3P mediated by the two three-enzyme complexes (i.e., TIM-LA_ALD-FBP and TIM-HA_ALD-FBP) and two combinations of the one two-enzyme complex (TIM-FBP) and one free HA_ALD or LA_ALD (Figure 3). The concentration of each enzyme component was 2 μM. The degree of substrate channelling was defined as the ratio of the initial reaction rate of the synthetic three-enzyme complex to the two-enzyme complex with a nonbound ALD at the same enzyme concentration. At 2.5 mM G3P, the initial F6P generation rate mediated by the three-enzyme complex containing LA_ALD (i.e., TIM-LA_ALD-FBP) was approximately 0.79 μM s^{-1}, approximately 7.5-fold higher than that of the two-enzyme complex plus the nonbound LA_ALD (Figure 3A). In contrast, the initial F6P generation rate mediated by the synthetic three-enzyme complex containing HA_ALD (i.e., TIM-HA_ALD-FBP) was approximately 0.82 μM s^{-1}, only 1.5-fold higher than that of the two-enzyme complex along with the nonbound HA_ALD (Figure 3B). This result indicated that the three-enzyme complex containing high-activity ALD exhibited lower degree of substrate channelling than the three-enzyme complex containing low-activity ALD. The degrees of substrate channelling of both of the synthetic enzyme complexes decreased as G3P concentration increased, suggesting that the substrate channelling may be more important under low substrate reaction conditions (Figure 4).

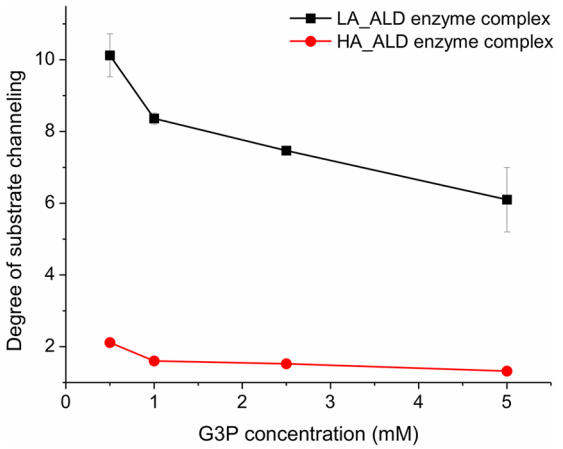

Figure 4. Degree of substrate channeling for the two three-enzyme complexes in terms of substrate concentration.

The apparent kinetic parameters of the three-enzyme complexes and the two-enzyme complex (TIM-FBP) along with the two nonbound ALDs were determined based on Michaelis–Menten kinetics (Supporting Information Figure 2). It was noted that apparent k_{cat} and K_m values of the free enzyme mixture (Table 1) were valid only for 2 μM of the noncomplexed enzyme mixture because of the nonlinear dependence of initial rate on enzyme concentration.[25] The three-enzyme complexes (TIM-LA_ALD-FBP and TIM-HA_ALD-FBP) both decreased K_m values compared to the

Table 1. Apparent Kinetic Parameters for the Two Three Enzyme Complexes and Two Non-complexed Enzyme Systems

name	K_m (mM)	k_{cat} (min^{-1})	k_{cat}/K_m (mM^{-1} min^{-1})
TIM-LA_ALD-FBP	0.48 ± 0.13	38.5 ± 4.3	80.8
LA_ALD[a] with TIM-FBP	1.51 ± 0.22	8.3 ± 0.6	5.5
TIM-HA_ALD-FBP	0.52 ± 0.15	42.4 ± 3.9	81.7
HA_ALD[a] with TIM-FBP	0.79 ± 0.08	34.0 ± 1.1	43.2

[a]The K_m and k_{cat} values of LA_ALD and HA_ALD were the same as those measured in the cases of LA_ALD with TIM-FBP and HA_ALD with TIM-FBP, respectively.

two-enzyme complex with the nonbound ALDs and increased k_{cat} values (Table 1). It was surprising that the catalytic efficiencies (k_{cat}/K_m) of the two three-enzyme complexes were comparable, being about 80 mM^{-1} min^{-1}, although their ratio of the specific activity of the annexed HA_ALD to LA_ALD was 5.

Substrate Channeling of the Different Ratio Enzyme Complexes. Cell-free synthetic biology allows us to easily control experimental conditions to investigate the clear relationship between inputs and outputs. Furthermore, we adjusted the ratio of LA_ALD to HA_ALD in the three-enzyme complexes from 3:1, 1:1 to 1:3 (Figure 5). For

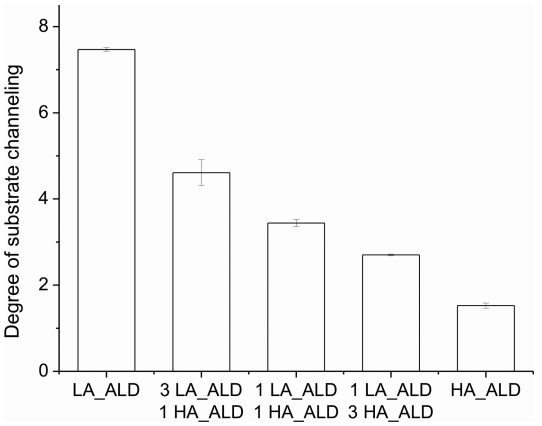

Figure 5. Degree of substrate channeling of the synthetic enzyme complexes containing a different ratio of LA_ALD to HA_ALD.

example, when the molar ratio of LA_ALD to HA_ALD was 3:1, the three-enzyme complex mixture contained 1.5 μM of TIM-LA_ALD-FBP enzyme complex and 0.5 μM of TIM-HA_ALD-FBP enzyme complex; the noncomplexed mixture was 2 μM of the two-enzyme complex (TIM-FBP), 1.5 μM of dockerin-free LA_ALD, and 0.5 μM of dockerin-free HA_ALD. The initial rate of the F6P formation was measured on 2.5 mM G3P at 60 °C. Clearly, the annexation of more high-activity ALD in the three-enzyme complexes decreased the degree of substrate channeling from 7.5 to 1.5 (Figure 5). These results strongly suggested that the construction of synthetic enzyme enzymes in cascade pathways could be a very important tool to accrelerate rate-limiting steps controlled by low-activity enzymes. Also, these result implied that the degree of substrate channeling depended on the enzyme choice.

In conclusion, the degrees of substrate channeling of the synthetic TIM-ALD-FBP complexes were investigated by the

dx.doi.org/10.1021/sb4000993 | ACS Synth. Biol. XXXX, XXX, XXX–XXX

Table 2. Strains and Plasmids

stains or plasmids	characteristics	ref
	E. coli	
Top10	*F⁻mcrA Δ(mrr-hsdRMS-mcrBC) φ80lacZΔM15 ΔlacX74 nupG recA1 araD139 Δ(ara-leu)7697 galE15 galK16 rpsL(StrR) endA1 λ-*	Invitrogen
BL21 Star (DE3)	F⁻*ompT hsd*SB (rB⁻mB⁻) *gal dcm rne131* (DE3)	Invitrogen
	Plasmids	
pET20b-cbm-scaf3	Amp^R, mini-scaffoldin expression cassette containing a CBM3 module from *C. thermocellum* CipA and three different cohesins from *C. thermocellum*, *C. cellulovorans*, and *R. flavefaciens*	17
pET20b-tim-ctdoc	Amp^R, ttctim-ctdoc expression cassette containing TIM module (TTC0581) from *T. thermophiles* and the dockerin module from *C. thermocellum*	17
pET20b-tmald-ccdoc	Amp^R, tmald-ccdoc expression cassette containing TmALD module (TM0273) from *T. maritime* and the dockerin module from *C. cellulovorans*	17
pET20b-ttcald-ccdoc	Amp^R, ttcald-ccdoc expression cassette containing TtcALD module (Ttc1414) from *T. thermophiles* and the dockerin module from *C. cellulovorans*	this work
pET20b-fbp-rfdoc	Amp^R, fbp-rfdoc expression cassette containing FBP module (TM1415) from *T. maritime* and the dockerin module from *R. flavefaciens.*	17
pET28a-tmald	Kana^R, tmald expression cassette containing TmALD protein, which was purified based on the C-terminal 6× His tag	gifted by J. J. Zhong
pET20a-ttcald	Amp^R, ttcald expression cassette containing TtcALD protein, which was purified based on the C-terminal 6× His tag	this study

annexation of high-activity and low-activity ALDs at different ratios. The annexation of high-activity enzyme decreased the degree of substrate channeling greatly. This study provided a clear evidence whether substrate channeling was observed or not depended on enzyme choice.

METHODS

Chemicals. All chemicals were reagent grade or higher, purchased from Sigma (St. Louis, MO) or Fisher Scientific (Pittsburgh, PA), unless otherwise noted. Microcrystalline cellulose—Avicel PH105 (20 μm)—was purchased from FMC (Philadelphia, PA). Large accessibility regenerated amorphous cellulose (RAC) was prepared from Avicel through cellulose dissolution and precipitation as previously described.[37] The PCR enzyme was Phusion DNA polymerase from New England Biolabs (Ipswich, MA). The oligonucleotides were synthesized by Integrated DNA Technologies (Coraville, IA).

Strains and Medium. *Escherichia coli* Top10 was used as a host cell for DNA manipulation, and *E. coli* BL21 Star (DE3) (Invitrogen, Carlsbad, CA) was used as a host cell for recombinant protein expression. The Luria−Bertani (LB) medium was used for *E. coli* cell culture and recombinant protein expression. The final concentrations of antibiotics for *E. coli* were 100 mg/L ampicillin or 50 mg/L kanamycin.

Construction of Plasmids. The plasmids are summarized in Table 2. The plasmids pET20b-cbm-scaf3, pET20b-tim-ctdoc, pET20b-tmald-ccdoc, pET28a-tmald and pET20b-fbp-rfdoc were constructed as described previously.[17,27]

Plasmid pET20b-ttcald had an expression cassette containing the ttc*ald* gene (Ttc1414) from *T. thermophilus* HB27. *The* 918-bp DNA fragment containing the open reading frame (ORF) of the fructose-bisphosphate aldolase (Ttc1414) was amplified by PCR from the genomic DNA of *Thermus thermophilus* HB27 using a pair of primers (forward primer: 5′-TAACT TTAAG AAGGA GATAT ACATA TGCTG GTAAC GGGTC TAGAG ATCT-3′; reverse primer: 5′-AGTGG TGGTG GTGGT GGTGC TCGAG AGCCC GCCCC ACGGA GCCGA AAAGC-3′). The vector backbone of pET20b was amplified by PCR using a pair of primers (forward primer: 5′-GCTTT TCGGC TCCGT GGGGC GGGCT CTCGA GCACC ACCAC CACCA CCACT-3′; reverse primer: 5′-AGATC TCTAG ACCCG TTACC AGCAT ATGTA TATCT CCTTC TTAAA GTTAA-3′). The PCR products were purified using the Zymo Research DNA Clean & Concentrator Kit (Irvine, CA). The insertion DNA fragment and vector backbone were assembled by prolonged overlap extension PCR (POE-PCR),[38] and then the POE-PCR product (DNA multimer) was directly transformed into *E. coli* TOP10 cells, yielding the desired plasmid.

Plasmid pET20b-ttcald-ccdoc had an expression cassette containing the ttc*ald* gene (Ttc1414) from *T. thermophilus HB27* and a dockerin module from endoglucanase EngE (943−1030 amino acids, GenBank Accession number: AAD39739.1) of *Clostridium cellulovorans.* The DNA fragment containing ttc*ald* gene was amplified with a pair primerd (forward primer: 5′-ACTTT AAGAA GGAGA TATAC ATATG CTGGT AACGG GTCTA GAGAT CTTGC-3′; reverse primer: 5′-CTTGG ATTCC TGGTA ATACC TTACC AGCCC GCCC CACGG AGCCG AAAAG C-3′) based on the genomic DNA of *T. thermophilus* HB27; the pET20b-ccdoc vector backbone was amplified with a pair of primers (forward primer: 5′-GCTTT TCGGC TCCGT GGGGC GGGCT GGTAA GGTAT TACCA GGAAT CCAAG-3′; reverse primer: 5′-GCAAG ATCTC TAGAC CCGTT ACCAG CATAT GTATA TCTCC TTCTT AAAGT-3′) based on the template of plasmid pET20b-tmald-ccdoc. Plasmid pET20b-ttcald-ccdoc was assembled based on the above two DNA fragments by using restriction enzyme-free, ligase-free and sequence-independent Simple Cloning.[38] All the plasmid sequences were validated by DNA sequencing.

Recombinant Protein Expression and Purification. The strains *E. coli* BL21 Star (DE3) containing the protein expression plasmids were cultivated in the LB medium supplemented with 1.2% glycerol at 37 °C. When A_{600} reached about 0.75, 100 μM isopropyl-beta-D-thiogalactopyranoside (IPTG, a final concentration) was added and the cultivation temperature was decreased to 16 °C for ∼16 h. After centrifugation, the cell pellets were resuspended in a 50 mM HEPES buffer (pH 8.5) containing 1 mM $CaCl_2$ and 50 mM NaCl. The cells were lysed by ultrasonication. The cell extracts (10 μL) were loaded into 12% SDS-PAGE to check the expression level of the four proteins. Protein purification of His-tag containing protein was conducted routinely by using Ni-NTA resins.[39]

One-Step Metabolon Purification and Immobilization. After roughly estimation of each targeted protein expression

dx.doi.org/10.1021/sb4000993 | ACS Synth. Biol. XXXX, XXX, XXX−XXX

level by SDS-PAGE, 20 mL of the cell lysate supernatant of TIM-CtDoC, 10 mL of the cell lysate supernatant of TmALD-CcDoc or TtcALD-CcDoc, 10 mL of the cell lysate supernatant of FBP-RfDoc were mixed with 6 mL of the cell lysate supernatant of mini-scaffoldin CBM3-CtCoh-CcDoc-RfCoh (i.e., CBM-Scaf3), making sure that TIM-CtDoc, TmALD-CcDoc or TtcALD-CcDoc, FBP-RfDoc were a little in excess compared to CBM-Scaf3. Then, 100 mg RAC was used to absorb CBM3-containing enzyme complex at room temperature for 5 min. After centrifugation at 3710 g for 10 min, the RAC pellet was washed in 20 mL of 100 mM HEPES (pH 7.5) containing 50 mM NaCl and 1 mM $CaCl_2$ three times. After centrifugation at 5000 rpm for 10 min, the RAC pellet was obtained as immobilized enzyme complex. Then, 200 μg of pellet was resuspended in 40 μL of 1× SDS loading buffer. After boiling for 2 min, 10 μL of the supernatant was loaded into 12% SDS-PAGE to check the interaction between mini-scaffoldin and dockerin containing enzymes.

Enzymatic Activity Assays. The activity of TIM was measured in 100 mM HEPES pH 7.5 containing 10 mM $MgCl_2$, 0.5 mM $MnCl_2$ at 60 °C for 5 min containing 2 mM D-glyceraldehyde 3-phosphate. The reaction sample (65 μL) was withdrawn at indicated time intervals. The reactions were terminated by adding 35 μL of 1.88 M perchloric acid. After centrifugation, the pH of the supernatant was neutralized with 13 μL of 5 M KOH. The product dihydroxyacetone phosphate was measured by using glycerol 3-phosphate dehydrogenase in the presence of 0.15 mM NADH at 37 °C. ALD activity was assayed in 100 mM HEPES (pH 7.5) containing 10 mM $MgCl_2$ and 0.5 mM $MnCl_2$ at 60 °C for 5 min with 5 mM of D-glyceraldehyde 3-phosphate in presence of excess TIM, FBP, and PGI. The specific acivity of ALD was measured at its concentration of 2 μM. The reaction was stopped with $HClO_4$ and neutralized with KOH. The product glucose 6-phosphate was analyzed at 37 °C with liquid glucose reagent set (Pointe Scientific). *T. maritima* FBP activity was determined based on the release of phosphate.[40] The overall reaction activity of three enzymes was measured in a 200 mM HEPES buffer (pH 7.5) containing 10 mM $MgCl_2$, 0.5 mM $MnCl_2$, 1 mM $CaCl_2$, and 2.5 mM glycerealdehyde-3-phosphate (G3P) at 37 °C. In order to determine the substrate channeling, two enzyme systems were tested to determine the enzymatic activity: RAC immobilized three enzyme complex and dockerin-free ALD with RAC immobilized two enzyme complex containing TIM and FBP. For the activity assay, 2 μM of the enzyme systems were used. The reaction systems contained only enzymes or substrates were performed as negative controls. The reaction was stopped with $HClO_4$ and neutralized with KOH. The production of fructose-6-phosphate (F6P) was measured by using a glucose hexokinase/glucose-6-phosphate dehydrogenase assay kit (Pointe Scientific, Canton, MI) supplemented with the recombination phosphoglucose isomerase.[41] The kinetic parameters of two enzymes systems were determined from the overall enzymatic activities at different G3P concentrations Michaelis−Menten equation.

Other Assays. Protein mass concentration was measured by the Bio-Rad Bradford protein dye reagent method (Bio-Rad, Hercules, CA) with bovine serum albumin as a reference. The protein mass based on the Bradford method was calibrated by their absorbance (280 nm) in 6 M guanidine hydrochloride. The purity of protein samples was examined by 12% SDS-PAGE. The SDS-PAGE gel was stained by Bio-Rad Bio-Safe Colloidal Coomassie Blue G-250. The intensity of the band in the gel was analyzed with Quantity One (Bio-Rad, Version 4.6.7).

■ ASSOCIATED CONTENT

Supporting Information

Supplementary Figures 1−3 used in the work. This material is available free of charge via the Internet at http://pubs.acs.org.

■ AUTHOR INFORMATION

Corresponding Author

*Tel: 540-231-7414. Fax: 540-231-3199. E-mail: ypzhang@vt.edu.

Notes

The authors declare no competing financial interest.

■ ACKNOWLEDGMENTS

The authors are thankful for the support from the Biological System Engineering Department of Virginia Tech. This work was mainly based on work supported by the DOE ARPA-E Petro award to P.Z.

■ REFERENCES

(1) You, C., Chen, H., Myung, S., Sathitsuksanoh, N., Ma, H., Zhang, X.-Z., Li, J., and Zhang, Y.-H. P. (2013) Enzymatic transformation of nonfood biomass to starch. *Proc. Natl. Acad. Sci. U.S.A. 110*, 7182−7187.

(2) Andrianantoandro, E., Basu, S., Karig, D. K., and Weiss, R. (2006) Synthetic biology: New engineering rules for an emerging discipline. *Mol. Syst. Biol. 2*, 28.

(3) Rollin, J. A., Tam, T. K., and Zhang, Y.-H. P. (2013) New biotechnology paradigm: Cell-free biosystems for biomanufacturing. *Green Chem. 15*, 1708−1719.

(4) You, C., and Zhang, Y. H. P. (2013) Cell-free biosystems for biomanufacturing. In *Adv. Biochem. Eng. Biotechnol.* (Zhong, J.-J., Ed.), pp 89−119, Springer, Berlin Heidelberg.

(5) Eric Hodgman, C., and Jewett, M. C. (2012) Cell-free synthetic biology: Thinking outside the cell. *Metab. Eng. 14*, 261−269.

(6) Guterl, J.-K., Garbe, D., Carsten, J., Steffler, F., Sommer, B., Reiße, S., Philipp, A., Haack, M., Rühmann, B., Koltermann, A., Kettling, U., Brück, T., and Sieber, V. (2012) Cell-free metabolic engineering: Production of chemicals by minimized reaction cascades. *ChemSusChem 5*, 2165−2172.

(7) Harris, D. C., and Jewett, M. C. (2012) Cell-free biology: Exploiting the interface between synthetic biology and synthetic chemistry. *Curr. Opin. Biotechnol. 23*, 672−678.

(8) Ardao, I., Hwang, E., and Zeng, A.-P. (2013) In *Adv. Biochem. Eng. Biotechnol.*, pp 1−32, Springer, Berlin Heidelberg.

(9) Schoffelen, S., and van Hest, J. C. M. (2012) Multi-enzyme systems: Bringing enzymes together in vitro. *Soft Matter 8*, 1736−1746.

(10) Zhang, Y. H. P. (2011) Substrate channeling and enzyme complexes for biotechnological applications. *Biotechnol. Adv. 29*, 715−725.

(11) Conrado, R. J., Wu, G. C., Boock, J. T., Xu, H., Chen, S. Y., Lebar, T., Turnšek, J., Tomšič, N., Avbelj, M., Gaber, R., Koprivnjak, T., Mori, J., Glavnik, V., Vovk, I., Benčina, M., Hodnik, V., Anderluh, G., Dueber, J. E., Jerala, R., and DeLisa, M. P. (2012) DNA-guided assembly of biosynthetic pathways promotes improved catalytic efficiency. *Nucleic Acids Res. 40*, 1879−1889.

(12) Fu, J., Liu, M., Liu, Y., Woodbury, N. W., and Yan, H. (2012) Interenzyme substrate diffusion for an enzyme cascade organized on spatially addressable DNA nanostructures. *J. Am. Chem. Soc. 134*, 5516−5519.

(13) Erkelenz, M., Kuo, C.-H., and Niemeyer, C. M. (2011) DNA-mediated assembly of cytochrome P450 BM3 subdomains. *J. Am. Chem. Soc. 133*, 16111−16118.

(14) Müller, J., and Niemeyer, C. M. (2008) DNA-directed assembly of artificial multienzyme complexes. *Biochem. Biophys. Res. Commun. 377*, 62−67.
(15) Wilner, O. I., Weizmann, Y., Gill, R., Lioubashevski, O., Freeman, R., and Willner, I. (2009) Enzyme cascades activated on topologically programmed DNA scaffolds. *Nat. Nano 4*, 249−254.
(16) Delebecque, C. J., Lindner, A. B., Silver, P. A., and Aldaye, F. A. (2011) Organization of intracellular reactions with rationally designed RNA assemblies. *Science 333*, 470−474.
(17) You, C., and Zhang, Y. H. P. (2013) Self-assembly of synthetic metabolons through synthetic protein scaffolds: One-step purification, co-immobilization, and substrate channeling. *ACS Synth. Biol. 2*, 102−110.
(18) Dueber, J. E., Wu, G. C., Malmirchegini, G. R., Moon, T. S., Petzold, C. J., Ullal, A. V., Prather, K. L. J., and Keasling, J. D. (2009) Synthetic protein scaffolds provide modular control over metabolic flux. *Nat. Biotechnol. 27*, 753−759.
(19) Hirakawa, H., and Nagamune, T. (2010) Molecular assembly of P450 with ferredoxin and ferredoxin reductase by fusion to PCNA. *ChemBioChem 11*, 1517−1520.
(20) Jandt, U., You, C., Zhang, Y.-H. P., Zeng, A. (2013) Compartmentalization and metabolic channeling for multienzymatic biosynthesis: Practical strategies and modeling approaches. In *Adv. Biochem. Eng. Biotechnol.* DOI: 10.1007/10_2013_221.
(21) Chen, A. H., and Silver, P. A. (2012) Designing biological compartmentalization. *Trends Cell Biol. 22*, 662−670.
(22) Sheldon, R. A., and van Pelt, S. (2013) Enzyme immobilisation in biocatalysis: Why, what, and how. *Chem. Soc. Rev. 42*, 6223−6235.
(23) Bulow, L., Ljungcrantz, P., and Mosbach, K. (1985) Preparation of a soluble bifunctional enzyme by gene fusion. *Nat. Biotechnol. 3*, 821−823.
(24) Agapakis, C. M., Ducat, D. C., Boyle, P. M., Wintermute, E. H., Way, J. C., and Silver, P. A. (2010) Insulation of a synthetic hydrogen metabolism circuit in bacteria. *J. Biol. Eng. 4*, 3.
(25) You, C., Myung, S., and Zhang, Y. H. P. (2012) Facilitated substrate channeling in a self-assembled trifunctional enzyme complex. *Angew. Chem., Int. Ed. 51*, 8787−8790.
(26) Liu, Y., Du, J., Yan, M., Lau, M. Y., Hu, J., Han, H., Yang, O. O., Liang, S., Wei, W., Wang, H., Li, J., Zhu, X., Shi, L., Chen, W., Ji, C., and Lu, Y. (2013) Biomimetic enzyme nanocomplexes and their use as antidotes and preventive measures for alcohol intoxication. *Nat. Nano 8*, 187−192.
(27) Myung, S., and Zhang, Y. H. P. (2013) Non-complexed four cascade enzyme mixture: Simple purification and synergetic co-stabilization. *PLoS One 8*, e61500.
(28) Schoffelen, S., Beekwilder, J., Debets, M. F., Bosch, D., and Hest, J. C. M. v. (2013) Construction of a multifunctional enzyme complex via the strain-promoted azide−alkyne cycloaddition. *Bioconjugate Chem. 24*, 987−996.
(29) Zhang, Y.-H. P., Evans, B. R., Mielenz, J. R., Hopkins, R. C., and Adams, M. W. W. (2007) High-yield hydrogen production from starch and water by a synthetic enzymatic pathway. *PLoS One 2*, e456.
(30) Martín del Campo, J. S., Rollin, J., Myung, S., Chun, Y., Chandrayan, S., Patiño, R., Adams, M. W. W., and Zhang, Y. H. P. (2013) High-yield production of dihydrogen from xylose by using a synthetic enzyme cascade in a cell-free system. *Angew. Chem., Int. Ed. 52*, 4587−4590.
(31) Ye, X., Wang, Y., Hopkins, R. C., Adams, M. W. W., Evans, B. R., Mielenz, J. R., and Zhang, Y.-H. P. (2009) Spontaneous high-yield production of hydrogen from cellulosic materials and water catalyzed by enzyme cocktails. *ChemSusChem 2*, 149−152.
(32) Sauvé, V., and Sygusch, J. (2001) Molecular cloning, expression, purification, and characterization of fructose-1,6-bisphosphate aldolase from *Thermus aquaticus*. *Protein Expression Purif. 21*, 293−302.
(33) Demishtein, A., Karpol, A., Barak, Y., Lamed, R., and Bayer, E. A. (2010) Characterization of a dockerin-based affinity tag: Application for purification of a broad variety of target proteins. *J. Mol. Recognit. 23*, 525−535.
(34) Zhang, Y. H. P., Cui, J., Lynd, L. R., and Kuang, L. R. (2006) A Transition from Cellulose Swelling to Cellulose Dissolution by *o*-Phosphoric Acid: Evidence from Enzymatic Hydrolysis and Supramolecular Structure. *Biomacromolecules 7*, 644−648.
(35) Hong, J., Ye, X., and Zhang, Y.-H. P. (2007) Quantitative determination of cellulose accessibility to cellulase based on adsorption of a nonhydrolytic fusion protein containing CBM and GFP with its applications. *Langmuir 23*, 12535−12540.
(36) Karpol, A., Barak, Y., Lamed, R., Shoham, Y., and Bayer, E. A. (2008) Functional asymmetry in cohesin binding belies inherent symmetry of the dockerin module: Insight into cellulosome assembly revealed by systematic mutagenesis. *Biochem. J. 410*, 331−338.
(37) Zhang, Y.-H. P., Cui, J., Lynd, L. R., and Kuang, L. R. (2006) A transition from cellulose swelling to cellulose dissolution by o-phosphoric acid: Evidence from enzymatic hydrolysis and supramolecular structure. *Biomacromolecules 7*, 644−648.
(38) You, C., Zhang, X.-Z., and Zhang, Y.-H. P. (2012) Simple cloning via direct transformation of PCR product (DNA multimer) to *Escherichia coli* and *Bacillus subtilis*. *Appl. Environ. Microbiol. 78*, 1593−1595.
(39) Wang, Y., Huang, W., Sathitsuksanoh, N., Zhu, Z., and Zhang, Y.-H. P. (2011) Biohydrogenation from biomass sugar mediated by *in vitro* synthetic enzymatic pathways. *Chem. Biol. 18*, 372−380.
(40) Myung, S., Wang, Y. R., and Zhang, Y.-H. P. (2010) Fructose-1,6-bisphosphatase from a hyper-thermophilic bacterium *Thermotoga maritima*: Characterization, metabolite stability, and its implications. *Proc. Biochem. 45*, 1882−1887.
(41) Myung, S., Zhang, X.-Z., and Zhang, Y.-H. P. (2011) Ultra-stable phosphoglucose isomerase through immobilization of cellulose-binding module-tagged thermophilic enzyme on low-cost high-capacity cellulosic adsorbent. *Biotechnol. Prog. 27*, 969−975.